SPE 9302

TECHNIQUES FOR FULLY IMPLICIT RESERVOIR SIMULATION

by Anthony D.K. Au, Alda Behie, Barry Rubin, and
Kaz Vinsome, Computer Modelling Group

This paper was presented at the 55th Annual Fall Technical Conference and Exhibition of the Society of Petroleum Engineers of AIME, held in Dallas, Texas, September 21-24, 1980.

ABSTRACT

This paper summarizes the methods that have been used to develop fully implicit and highly implicit reservoir simulators.

The techniques developed emphasize simplicity and clarity. The governing equations, written in fully implicit form are treated as functions. These coupled nonlinear functions are solved by Newtonian iteration, the derivatives of the Jacobian matrix being evaluated numerically. A procedure is described for the efficient evaluation of the Jacobian.

A technique is presented for avoiding variable substitution in variable bubble point problems. This is accomplished by means of a novel pseudo solution gas formulation.

An efficient method for including two-point upstream into fully implicit simulators, without increasing the Jacobian bandwidth, is described. The scheme is based on a fully implicit upstream mobility plus an explicit correction term derived from the two-point mobility formulation. In addition a new method called centralized upstream is given. The new method has less truncation error then two-point upstream, and is little more difficult to implement.

A modified Crank-Nicholson method is described for reducing the time truncation error associated with large time steps in implicit models. The modified version does not exhibit the usual stability problems associated with the Crank-Nicholson method on non-linear problems.

A section on well models shows how a simple enhancement of conventional well models can be used to account for the position of a well within a grid block. It is also shown how to introduce a multiblock well completion into an implicit simulator without destroying the block-banded form of the Jacobian, or without increasing the bandwidth.

An efficient iterative solution method is described for the sparse block-structured Jacobians. The method extends the SIP factorization to block form and uses minimizations and orthogonalizations to accelerate the convergence rate.

Several applications and examples are provided. A water coning example is included to show the stability and convergence characteristics of the Newtonian iteration. A vertical cross-section oil resaturation problem with variable bubble point is used to illustrate the pseudo solution gas formulation. The modified Crank-Nicholson method is applied to a one-dimensional Buckley-Leverett type problem.

References and illustrations at end of paper.

INTRODUCTION

It is well known that fully implicit methods are remarkably stable and can tolerate much larger time steps than those used in explicit formulations. However, fully implicit methods are not widely applied in large scale numerical problems such as oil reservoir simulation. The larger matrix bandwidth associated with fully implicit approach demands more computation effort per time step and computer core memory compared with explicit methods. Other considerations such as time truncation error associated with the large time step size and the difficulties in the implementation of higher order methods to reduce spatial truncation have also made the fully implicit method less attractive.

A collection of techniques for resolving these difficulties in fully implicit simulation is contained in this paper.

GENERAL CHARACTERISTICS OF NEWTONIAN ITERATION

The Newton algorithm is a well known iterative process for the numerical solution of equations. For a given function

$$f(x) = 0 \qquad \ldots (1)$$

the solution x is obtained by the iterative procedure

$$x^{k+1} = x^k - \frac{f(x^k)}{f'(x^k)} \quad \ldots (2)$$

starting from an initial estimate x°. The Newtonian iteration has second-order convergence characteristics. Given a proper choice of the initial estimate x°, convergence normally occurs rapidly.

In numerical reservoir simulation the solution at the previous time step is taken as the initial estimate. The convergence is generally obtained in 2 to 5 iterations. The stability of the Newtonian iteration is maintained even with large changes in the independent variables. An average saturation or molar fraction change of the order of 30% is common in fully implicit black oil or thermal simulations.

The work involved in the Newtonian iteration is quite high. For each iteration the functions and their derivatives have to be evaluated and the matrix inverted. The complexity associated with the analytical evaluation of the Jacobian matrix may be greatly reduced by a numerical approach. The derivative of the function $f(x_1, x_2, x_3)$ with respect to the dependent variable x_2 may be determined by

$$\frac{\partial f(x_1,x_2,x_3)}{\partial x_2} = \frac{f(x_1,x_2+\varepsilon,x_3) - f(x_1,x_2,x_3)}{\varepsilon} \quad \ldots (3)$$

where ε is a small number but large enough to result in a non-zero numerator in (3) when the derivative is non-zero. The numerical evaluation of each derivative in the Jacobian matrix requires two function evaluations.

The computational work required to construct the Jacobian matrix can be reduced with a special Jacobian building technique described in a subsequent section. The combination of using numerical derivatives, Jacobian building method and an efficient matrix inversion procedure makes the Newtonian iteration scheme an effective solution method.

Two examples to show the stability and convergence characteristics of the Newtonian iteration are the oil resaturation problem given in Appendix A and the water coning problem given in Appendix B.

PSEUDO SOLUTION GAS

Pseuso solution gas is a technique whereby variable bubble point black oil problems can be handled without any variable substitution in the numerical solution procedure.

The technique involves replacing the true solution gas-oil ratio R_s by a pseudo solution gas-oil ratio R_{sp} defined as

$$R_{sp} = \Phi(S_g) \cdot R_s \quad \ldots (4)$$

where

R_s = true solution gas-oil ratio assuming an unlimited supply of free gas. R_s is a function of pressure, but has no discontinuity in slope at the bubble point.

$\Phi(S_g)$ = the pseudo function which is defined as

$$\Phi = 1 \text{ for } S_g > \varepsilon \quad \ldots (5)$$

$$\Phi = \frac{S_g}{\varepsilon} \text{ for } S_g \leq \varepsilon \quad \ldots (6)$$

and ε is a small number of order 10^{-4}. If any gas is present the pseudo function has a value of unity, and so does nothing. As the gas saturation decreases towards zero the pseudo solution gas-oil ratio suddenly decreases. Further free gas is then prevented from going into solution, and a small gas saturation between 0 and ε is maintained in the system.

A typical black oil simulation would then involve the solution of three conservation equations; gas, oil, and water conservation in the three primary variables; pressure, oil saturation, and water saturation. It is equally possible to solve oil, gas, and water conservation equations in the primary variables of pressure, gas saturation, and water saturation.

There is no need for any variable substitution. In the above procedure there is no unique bubble point as it depends on the amount of gas present. R_s is a monotonic function of pressure P, and the oil formation volume factor should be expressed as a monotonic function of R_{sp}.

Instead of gas disappearing completely when the pressure rises above the bubble point, a small gas saturation is maintained. This can be made as small as possible by a slight redefinition of the pseudo function

$$\Phi = 1 \text{ for } S_g \geq \varepsilon(1-c) \quad \ldots (7)$$

$$\Phi = (S_g + c\varepsilon)/\varepsilon \text{ for } S_g < \varepsilon(1-c) \quad \ldots (8)$$

$$c = \frac{R_{si}}{R_s(P_i)} \quad \ldots (9)$$

where

R_{si} = initial solution gas-oil ratio

P_i = initial pressure

c is a number between 0 and 1, and with the above definitions the gas saturation is identically zero at the initial bubble point. If the pressure rises above the initial bubble point pressure small negative gas saturations will be calculated.

An example of a variable bubble point problem using the pseudo solution gas formulation is given in Appendix A.

SPATIAL TRUNCATION

Fully implicit simulators generally use single-point upstream mobilities. Inclusion of two-point upstream mobilities would drastically increase the bandwidth of the Jacobian matrix, if it were done in a fully implicit manner. However, in many cases the spatial truncation error from single-point upstream is unacceptable. A compromise is made

$$\lambda_{u+\frac{1}{2}}^{N+1} = \lambda_u^{N+1} + \frac{\Delta x}{2} \frac{\partial \lambda^N}{\partial x} \quad \ldots (10)$$

where

$\lambda_{u+\frac{1}{2}}$ = interblock mobility

λ_u = upstream mobility

N = time level

The upstream mobility is taken implicitly and the slope part explicitly. For two-point upstream the slope part is given by

$$\frac{\partial\lambda}{\partial x}^N = \frac{\lambda_u^N - \lambda_{uu}^N}{\Delta x} \quad \ldots (11)$$

where λ_{uu}^N is the two-point upstream value.

The slope is constrained such that the interblock mobility lies between the upstream and downstream mobilities

$$\min |\lambda_u, \lambda_d| \leq \lambda_{u+\frac{1}{2}}^N \leq \max |\lambda_u, \lambda_d| \quad \ldots (12)$$

No problems have been observed with this formulation, although part of it is explicit. Updation of the slope during each Newtonian iteration gave no significant difference in results. However it is better to leave the slope evaluation at the old time level as updation can slow down the rate of convergence of the Newtonian iteration.

There are other alternatives to evaluating the slope by two-point upstream. A simple one, which is better than two-point upstream, is centralized upstream.

$$\frac{\partial\lambda}{\partial x}^N = \frac{\lambda_d^N - \lambda_{uu}^N}{2\Delta x} \quad \ldots (13)$$

When using centralized upstream, in addition to the constraints (12), another set of constraints is required on the opposite face of the upstream block. Define

$$\lambda_{u-\frac{1}{2}}^N = \lambda_u^N - \frac{\Delta x}{2} \cdot \frac{(\lambda_d - \lambda_{uu})}{2\Delta x} \quad \ldots (14)$$

then the slope is constrained such that

$$\min |\lambda_{uu}, \lambda_u| \leq \lambda_{u-\frac{1}{2}}^N \leq \max |\lambda_{uu}, \lambda_u| \quad \ldots (15)$$

An example given in Appendix C showed the truncation error for centralized upstream to be slightly less than for two-point upstream. No stability problems have been observed with the explicit part of the interblock mobility. On all the simulation runs performed to date, centralized upstream was better than two-point upstream.

TIME TRUNCATION

The standard implicit finite-difference representation of the parabolic equation

$$\frac{\partial^2 u}{\partial x^2} = \frac{\partial u}{\partial t} \quad \ldots (16)$$

is

$$\left(\frac{\Delta^2 U}{\Delta X^2}\right)^{N+1} = \frac{U^{N+1} - U^N}{\Delta T} \quad \ldots (17)$$

Equation (17) is only first order correct in time with truncation error

$$E_I = \Delta T\left(\frac{1}{2}\frac{\partial^2 u}{\partial t^2} - \frac{\partial^3 u}{\partial x^2 \partial t}\right) - \frac{1}{12}\Delta X^2 \frac{\partial^4 u}{\partial x^4} + \Delta T^2\left(\frac{1}{6}\frac{\partial^3 u}{\partial t^3} - \frac{1}{2}\frac{\partial^4 u}{\partial x^2 \partial t^2}\right) + \ldots \quad \ldots (18)$$

Similarly the standard explicit method for representing equation (16) using finite-difference is

$$\left(\frac{\Delta^2 U}{\Delta X^2}\right)^N = \frac{U^{N+1} - U^N}{\Delta T} \quad \ldots (19)$$

Equation (19) is only first order correct in time with truncation error

$$E_E = -\Delta T\left(\frac{1}{2}\frac{\partial^2 u}{\partial t^2}\right) - \frac{1}{12}\Delta X^2 \frac{\partial^4 u}{\partial x^4} + \Delta T^2\left(\frac{1}{6}\frac{\partial^3 u}{\partial t^3}\right) + \ldots \quad \ldots (20)$$

For most reservoir simulation purposes using explicit techniques, the first order accuracy in time is adequate. However, when using fully implicit simulators where large time steps are used the time truncation can become important.

One method for discretizing equation (16), which is second order accurate in time, is the Crank-Nicholson (C-N) method

$$\frac{1}{2}\left(\frac{\Delta^2 U}{\Delta X^2}\right)^{N+1} + \frac{1}{2}\left(\frac{\Delta^2 U}{\Delta X^2}\right)^N = \frac{U^{N+1} - U^N}{\Delta T} \quad \ldots (21)$$

The truncation error for equation (21) is

$$E_{CN} = -\frac{1}{12}\Delta X^2 \frac{\partial^4 u}{\partial x^4} + \Delta T^2\left(\frac{1}{6}\frac{\partial^3 u}{\partial t^3} - \frac{1}{4}\frac{\partial^4 u}{\partial x^2 \partial t^2}\right) + \ldots \quad \ldots (22)$$

The C-N method is guaranteed to be unconditionally stable for the linear case; however, stability is not guaranteed for the nonlinear case. It is primarily for this reason that the C-N method has not been extensively applied to reservoir simulation[1].

The Crank-Nicholson method can be generalized by replacing the 0.5 weighting factors by a variable factor ω

$$\omega\left(\frac{\Delta^2 U}{\Delta X^2}\right)^{N+1} + (1-\omega)\left(\frac{\Delta^2 U}{\Delta X^2}\right)^N = \frac{U^{N+1} - U^N}{\Delta T} \quad \ldots (23)$$

with the truncation error

$$E_{GCN} = \Delta T\left(\frac{1}{2}\frac{\partial^2 u}{\partial t^2} - \omega\frac{\partial^3 u}{\partial x^2 \partial t}\right) - \frac{1}{12}\Delta X^2 \frac{\partial^4 u}{\partial x^4} + \Delta T^2\left(\frac{1}{6}\frac{\partial^3 u}{\partial t^3} - \frac{\omega}{2}\frac{\partial^4 u}{\partial x^2 \partial t^2}\right) + \ldots \quad \ldots (24)$$

The truncation error of the generalized Crank-Nicholson method reduces to that of the implicit method when ω equals 1 and to that of the C-N method when ω equals $\frac{1}{2}$.

For nonlinear problems, stability can be achieved by increasing the value of ω towards 1. The percentages of the fully implicit first order time truncation error associated with each ω are

ω	% First Order Error
0.50	0.0
0.55	10.0
0.60	20.0
0.65	30.0
0.75	50.0
1.00	100.0

Some results on the application of the generalized Crank-Nicholson method are given in Appendix D.

WELL MODELS

In most reservoir simulators the injection or production wells are represented as source and sink terms in the mathematical formulation. The function of a well model is to relate the magnitude of the source and sink term to the wellbore flow and to the flow from surrounding grid blocks. In this section we shall describe a simple enhancement of the conventional well models to account for the position of a well within a grid block. We shall also introduce a method of modelling multiblock well completion in a fully implicit simulator without increasing the bandwidth of the matrix.

Areal Effects

The well inflow performance is given by

$$q = \frac{2\pi\lambda k h f (P_i - P_b)}{[\ln c_g \frac{r_e}{r_w} + S]} \quad \ldots (25)$$

$$r_e = \sqrt{\frac{\Delta x \Delta y}{\pi f}} \quad \ldots (26)$$

λ = fluid mobility

k = absolute permeability

h = net thickness

f = well fraction

P_i = grid block pressure

P_b = wellbore pressure

c_g = geometrical factor

r_e = effective radius

r_w = wellbore radius

S = skin

q = fractional well rate

Peaceman[2] introduced the geometrical factor c_g to account for the fact that P_i is not necessarily equal to the pressure at the effective radius. Peaceman[2] only considered a well at the centre of a square grid block, and defined the effective radius as

$$r_e = \Delta x \quad \ldots (27)$$

In equation (26) we have introduced a factor π so that r_e is more consistent with the idea of using an effective block radius as has been done previously[3]. In addition we have introduced the well fraction f, which reduces the sensitivity of c_g to the geometrical location of the well within the grid block. Thus the definition of c_g used here differs from that of Peaceman[2] by the factor $\sqrt{\pi f}$. For a well at the centre of a grid block Peaceman[2] found that the geometrical factor was close to $e^{-\pi/2}$ or 0.21. For the definition adopted here

$$c_g = \sqrt{\pi}\, e^{-\pi/2} = 0.37 \quad \ldots (28)$$

In general we shall see that for various geometries c_g is around 0.5.

As an example we shall derive the geometrical factor for a quarter well at the corner of a grid block, as shown in Figure 1(f). Such a situation is common when modelling five-spot symmetry elements.

Assuming single-phase radial flow into the well (which is a quarter well)

$$P(r) - P_w = \frac{q\mu[\ln r/r_w + S]}{2\pi k h f} \quad \ldots (29)$$

At points j and ℓ

$$r_j = r_\ell = \frac{\sqrt{10}\,\Delta}{2} \quad \ldots (30)$$

From finite-difference and symmetry, the flow from the surrounding blocks into the well blocks is given by

$$q = \frac{2 k h}{\mu}(P_j - P_i) \quad \ldots (31)$$

Eliminating P_j between these equations gives

$$q = \frac{2\pi k h f}{\mu} \frac{(P_i - P_w)}{[\ln \frac{\sqrt{10}\, e^{-\pi f}\,\Delta}{2r_w} + S]} \quad \ldots (32)$$

which is consistent with (25) if

$$c_g = \frac{\sqrt{10\pi f}\, e^{-\pi f}}{2} = 0.64 \quad \ldots (33)$$

Other geometries can also be calculated. Figure 1 indicates the geometrical factors for some of the common cases. To obtain some of these results it is necessary to use the method of images. In Figure 1 it is assumed that the grid nodes are at the centre of the blocks. In radial coordinates r_e is defined as the radius of the first block, the grid node is assumed to be at $r_e/2$, and c_g can be evaluated directly from (25) by assuming P_i lies on the logarithmic inflow function.

Vertical Effects

When a production well, represented by sink terms extends through several grid blocks, the wellbore problem becomes complex. Firstly, a model is required to account for the wellbore pressure drop. Secondly, when the overall production rate of the well is specified by external constraints, a model for allocating production among grid blocks is required. We shall consider the pressure constrained well and the rate constrained well separately.

Pressure Constrained Wells

In order to simplify calculations this model divides the wellbore into two distinct regions. The first region represents the portion of the well from the reservoir to the surface, the second represents the portion of the well that intersects the reservoir. It is assumed the effects of pressure drop in the first section need not be modelled[4].

In the second section, it is assumed the pressure drops due to friction and inertial losses are negligible compared to the gravity head. The wellbore pressure distribution is then equal to the specific weight contribution or

$$\frac{\partial P}{\partial z} = \bar{\rho} g \qquad \ldots (34)$$

where

$\bar{\rho} = S_g \rho_g + S_o \rho_o + S_w \rho_w$

S_g = wellbore gas saturation

S_o = wellbore oil saturation

S_w = wellbore water saturation

ρ_j = density of phase j

ρg = wellbore gradient $\frac{psi}{ft}$

The bore pressure of block i within a multiblock completion well is

$$P_i = P_b - \int_{z_b}^{z_i} \bar{\rho} g dz \qquad \ldots (35)$$

It is possible to determine $\bar{\rho}$ using empirical multiphase flow calculations[5]. However for most wells $\int \bar{\rho} g dz$ is small over the producing zone compared to the drawdown. The assumption of constant ρ introduces only minor error. Equation (35) reduces to

$$P_i = P_b - \sum_{j=2}^{i} (\bar{\rho} g_{j-1}) \frac{\Delta z_{j-1} + \Delta z_j}{2} \qquad \ldots (36)$$

where

$P_b = P_1$ = bottom hole pressure

Δz_j = vertical length of wellbore in block j

The pressure gradient along the wellbore can also be estimated[6].

Rate Constrained Wells

The algorithm used to distribute a desired multiblock well production rate (Q_{mb}) among the wellbore grid blocks assumes that:

$$Q_{mb} = \sum_{i=1}^{NBW} \sum_{j=1}^{NP} T_{ij} \left(P_i - \left(P_b - \left[\int_{z_b}^{z_i} \bar{\rho} g \partial z\right]\right)\right) \qquad \ldots (37)$$

or

$$Q_{mb} = \sum_{i=1}^{NBW} \sum_{j=1}^{NP} T_{ij} \left(P_i - \left(P_b - Head_i\right)\right) \qquad \ldots (38)$$

where

$Head_i$ represents the expression in square brackets

NBW = number of blocks along the wellbore

NP = number of phases

P_i = pressure of block i

T_{ij} = transmissibility of phase j in block i

An expression for P_b can be obtained from (38)

$$P_b = \frac{\sum_{i=1}^{NBW} \sum_{j=1}^{NP} T_{ij} (P_i + Head_i) - Q_{mb}}{\sum_{i=1}^{NBW} \sum_{j=1}^{NP} T_{ij}} \qquad \ldots (39)$$

Equation (39) has been used in various simulators. However, the efficient implementation of this equation in a fully implicit simulator is not simple.

In order to maintain the second order convergence characteristics of the Newtonian iteration, the flow rate for each phase in each grid block, $Q_{i\ell}^{k+1}$, which is derived from equation (39) should be calculated fully implicitly. There would be contributions to the Jacobian matrix from all blocks in the multiblock completion well. This would increase the bandwidth of the Jacobian matrix and increase computation time. To circumvent this problem an approximation to $Q_{i\ell}^{k+1}$ has been developed which still maintains nearly second order convergence in the Newtonian iteration.

The approximation is based on two assumptions. The first is that

$$\sum_{m=1}^{NBW} \frac{\partial}{\partial P_m} Q_{i\ell}^{k} \, \delta P_m = 0 \qquad \ldots (40)$$

This can be shown to be identically true under the following conditions:

(1) $\delta P_m = P_m^{k+1} - P_m^k$ = constant for all m=1,...,NBW
i.e. pressure change in the well blocks is uniform over a Newtonian iteration,

and

(2) the dependence of transmissibilities on pressure is negligible.

The second assumption is that the total flow from each block is constant over a Newtonian iteration. That is

$$Q_{iT} = \sum_{\ell=1}^{NP} Q_{i\ell} = \text{constant} \qquad \ldots (41)$$

The equation for $Q_{i\ell}^{k+1}$ now becomes

$$Q_{i\ell}^{k+1} = Q_{i\ell}^{k} + \frac{\partial}{\partial S_\ell} Q_{i\ell}^{k} \, \delta S_\ell$$

$$= Q_{iT}^{k} \left(\frac{\lambda_{i\ell}}{\lambda_{iT}}\right)^k + Q_{iT}^{k} \frac{\partial}{\partial S_\ell} \left(\frac{\lambda_{i\ell}}{\lambda_{iT}}\right)^k \delta S_\ell \qquad \ldots (42)$$

Equation (42) has been implemented as follows. The total flow rate for each well block, Q_{iT}, and the well block phase distributions $\frac{\partial}{\partial S_\ell}\left(\frac{\lambda_{i\ell}}{\lambda_{iT}}\right)^k$ are

both calculated for the first η Newtonian iterations. For the remaining iterations the total rates previously determined are used and only the phase distributions are calculated. It was found that the calculated rates were insensitive to the value of η. A value of 2 or 3 is recommended. Furthermore, nearly second order convergence rates were obtained indicating that the assumptions are justified.

JACOBIAN CONSTRUCTION

The construction of the Jacobian matrix with numerical derivatives represents a significant portion of the computing time used in numerical reservoir simulation. Consider the finite-difference equation for a one-dimensional single-phase system written for block i

$$f_i = T_{i-\frac{1}{2}}^{N+1}(P_{i-1} - P_i)^{N+1} + T_{i+\frac{1}{2}}(P_{i+1} - P_i)^{N+1} - [(\phi_i\rho_i)^{N+1} - (\phi_i\rho_i)^N] - Q_i^{N+1} \quad \ldots (43)$$

Each row in the Jacobian matrix includes the derivative of f_i with respect to P_{i-1}, P_i and P_{i+1}. The derivatives, calculated numerically, require four function evaluations. If M blocks are used in the grid system equation (43) and the associated PVT properties must be evaluated 4M times.

A more efficient method of Jacobian construction is to make use of the relationship of interblock flow terms for adjacent grid blocks. Consider block j which is adjacent to block i,

$$f_j = T_{j-\frac{1}{2}}^{N+1}(P_{j-1} - P_j)^{N+1} + T_{j+\frac{1}{2}}(P_{j+1} - P_j)^{N+1} - [(\phi_j\rho_j)^{N+1} - (\phi_j\rho_j)^N] - Q_j^{N+1} \quad \ldots (44)$$

From Figure 2 it is clear that the derivative of equation (44) with respect to P_{j-1} is identical to the derivative of the second flow term in equation (43) with respect to P_i except the sign. Similarly for block m the derivative of f_m with respect to P_{m+1} is equivalent to the derivative of the first flow term in f_i with respect to P_i. Therefore, the off-diagonal entries in the Jacobian matrix are available by simply calculating the function and its derivative along the diagonal entries in parts and adding (or subtracting) the components in the appropriate locations in the same column of the matrix. The numerical derivatives are obtained by dividing entries in the matrix by the appropriate ΔP. This procedure is called a column oriented Jacobian construction. Since only two functional evaluations are needed, this procedure requires 50% of the work needed in the conventional row approach to Jacobian construction. The work reduction is 66% and 75% respectively for two- and three-dimensional problems.

ITERATIVE MATRIX INVERSION

In fully implicit, multiphase reservoir simulation, several equations must be solved simultaneously in each grid block. This results in a block-structured Jacobian matrix. An iterative method that is suitable for inverting this type of matrix and that is also powerful enough to solve difficult problems is critical to the performance of a fully implicit reservoir simulator.

A block iterative solution algorithm has been developed which encompasses two different options depending on the difficulty of the problem[6]. The solution algorithm consists of an approximate factorization followed by an acceleration technique. The different factorization options are described in reference 6. The acceleration technique is ORTHOMIN[7]. ORTHOMIN is a procedure which involves minimizations and orthogonalizations. The minimization step in ORTHOMIN guarantees that the algorithm can never diverge. The orthogonalizations mean that the algorithm should terminate in a finite number of iterations. Another advantage of this method is that no iteration parameters are required.

The block iterative algorithm has proven successful on a wide variety of problems including steam problems, in situ combustion problems, large black oil problems, and gas resaturation problems.

CONCLUSIONS

The techniques for fully implicit reservoir simulation presented in this paper have been applied to the in situ combustion, steamflooding and black oil simulators.

The programming effort required is moderate if numerical derivatives are used. With proper evaluation of the Jacobian and an efficient iterative matrix solution technique the overhead previously associated with the fully implicit method can be greatly reduced. New techniques have overcome the previous problems associated with large time steps and spatial truncation errors in highly implicit simulators.

We conclude that the fully implicit method, if implemented properly, is an effective numerical approach to reservoir simulation.

ACKNOWLEDGEMENT

This research was supported by the Alberta/Canada Energy Resources Research Fund administered by the Department of Energy and Natural Resources of the Province of Alberta.

NOMENCLATURE

B	- formation volume factor
C	- compressibility
c	- pseudo solution gas constant
c_g	- geometrical factor
E_E	- explicit truncation error
E_I	- implicit truncation error
E_{CN}	- Crank-Nicholson truncation error
E_{GCN}	- generalized Crank-Nicholson truncation error
E_g	- gas expansion factor
f	- function, well fraction
g	- gravity
H,h	- thickness
k	- absolute permeability
P	- pressure
Q	- flow rate

q - fractional well rate

r - radius

r_e - effective radius

r_w - well radius

R_s - solution gas-oil ratio

R_{sp} - pseudo solution gas-oil ratio

S - saturation, skin

T_{ij} - transmissibility of phase j in block i

t - time

u - dependent variable

x - independent variable

W - width

z - depth

ε - small constant

ρ - density

μ - viscosity

λ - fluid mobility

ϕ - porosity

Φ - pseudo function

ω - weighting factor

Subscripts

b - borehole

d - downstream grid block

i,j,ℓ,m - grid block index

g - gas

mb - multiblock

o - oil

r - rock, relative

u - upstream grid block

uu - two-point upstream grid block

w - water

Superscripts

k - iteration index

N - time step index

REFERENCES

1. K. Aziz and A. Settari, Petroleum Reservoir Simulation, Applied Science Publishers, London (1979).

2. Peaceman, D.W., "Interpretation of Well-Block Pressures in Numerical Reservoir Simulation," SPEJ (June 1978), 183-194.

3. Coats, K.H., George, W.D. and Marcum, B.E., "Three-Dimensional Simulation of Steamflooding," SPEJ (December 1974), 573-592.

4. Chappelear, J.E. and Williamson, A.S., "Representing Wells in Numerical Simulation - Theory and Implementation," SPE paper 7697, presented at the 5th SPE Symposium on Reservoir Simulation, Denver, Jan. 31-Feb. 2, 1979.

5. Govier, G.W. and Aziz, K., The Flow of Complex Mixtures in Pipes, Van Nostrand Reinhold, New York (1972).

6. Behie, A. and Vinsome, P.K.W., "Block Iterative Methods for Fully Implicit Reservoir Simulation," Paper to be presented at the SPE-AIME 55th Annual Technical Conference and Exhibition, Dallas, September 21-24, 1980.

7. Vinsome, P.K.W., "ORTHOMIN, An Iterative Method for Solving Sparse Sets of Simultaneous Linear Equations," Paper SPE 5729 presented at the SPE-AIME Fourth Symposium of Numerical Simulation of Reservoir Performance, Los Angeles, February 19-20, 1976.

8. Blair, P.M. and Weinaug, C.F., "Solution of Two Phase Flow Problems Using Implicit Difference Equations," Trans. SPE of AIME, Vol. 246 (December 1969), 417-424 (SPEJ).

9. Settari, A. and Aziz, K., "A Computer Model for Two-Phase Coning Simulation," SPEJ (June 1974), 221-236.

10. Grabowski, J.W., Vinsome, P.K.W., Lin, R.C., Behie, A. and Rubin, B., "A Fully Implicit General Purpose Finite-Difference Thermal Model for In Situ Combustion and Steam," Paper SPE 8396 presented at the SPE-AIME 54th Annual Fall Technical Conference and Exhibition, Las Vegas, September 1979.

APPENDIX A

OIL RESATURATION EXAMPLE

This problem was specifically designed to show the utility of the pseudo solution gas formulation. Almost every grid block experiences two transitions through the (variable) bubble point.

The system is a vertical cross-section. Dead oil is injected into the lower left hand grid block at constant rate, while production is at constant bottom hole flowing pressure from the lower right hand grid block.

The relative permeability and PVT data are given in Table 1. The oil is originally undersaturated. What happens in this run is that at first the production rate is larger than the injection rate, and so the reservoir is depleted. Apart from three grid blocks around the injector, each grid block experiences a transition through the bubble point, and gas is evolved. A gas cap is then formed by gravity segregation.

As the reservoir depletes, the production rate decreases so that the total downhole production rate of oil and gas approximately matches the injection rate. Dead oil then sweeps through the reservoir from the injector, and all the grid blocks where gas was evolved experience a second transition through the (variable) bubble point. These second transitions occur at a much lower pressure than the first.

Using maximum saturation changes of 5% this run took 60 time steps to reach 261 days, at which point all the gas had gone back into solution. This means that there were 94 transitions through the (variable)

bubble point in 60 time steps. Figure 3 shows the contours of solution gas ratio after 261 days.

There were an average of 3.4 Newtonian iterations/time step to reach a convergence tolerance of better than 0.001 in saturations in every grid block. After all the gas had redissolved the automatic selector increased the time step rapidly, and the run required a further 5 time steps to reach 500 days.

APPENDIX B

WATER CONING EXAMPLE

The sharp reduction in pore volumes of individual grid blocks around the wellbore and the convergent nature of the flow pattern make the coning model particularly subject to instability. We have chosen the problem of Blair and Weinaug[8] to test the stability of our fully implicit black oil model since it has been studied by many investigators. A summary of most of the previous work was reported by Settari and Aziz[9].

The data used here is identical to those given by Settari and Aziz[9] and it is not repeated here. Block centered grids are used with first grid block radius of 2.45 feet. The constant rate production well is located second block from the top of the reservoir. Water is injected at the outer most grid block on the bottom layer at constant rate to balance the production.

Two simulation runs were conducted with maximum time steps of 25 days and 100 days. The initial time step used in both runs was 5 days. The 25-day time step was reached and maintained after 36 days in the first run. In the second run the 100-day time step was reached at 428 days. Shortly before water breakthrough, at 728 days, the time step was reduced to 25 days by the automatic time step selection procedure[10] because the maximum saturation change had exceeded the 20% limit imposed. The 100-day time step was reached again at 1028 days. Another time step reduction occurred at 1128 days and the 100-day time step resumed at 1365 days. The average number of Newtonian iterations to reach a convergence tolerance of less than 0.001 in every grid block was 2.71 and 4.26 respectively for the 25-day and 100-day time steps.

The results of water-oil ratio (WOR) for the two runs and the result of Settari and Aziz[9] are shown in Figure 4. The WOR for both of our runs are almost equal. The data point is shown for the 100-day time step run only. The WOR at 2000 days for the time steps of 25 days and 100 days are 28.9% and 29.2% respectively.

Our results compared very well with those reported by Settari and Aziz[9].

APPENDIX C

MOBILITY APPROXIMATION METHODS

The problem is a one-dimensional Buckley-Leverett type displacement with straight line relative permeabilities and unit end point mobility ratio. This particular example is well known for the large amount of numerical dispersion exhibited by finite-difference solutions.

In Figure 5 the results are shown when 0.5 pore volumes have been injected. The analytical result is a 100% shock front at a fractional length of 0.5. The results show that single point upstream exhibits much more numerical dispersion than the other methods and centralized upstream shows the least numerical dispersion.

APPENDIX D

GENERALIZED CRANK-NICHOLSON EXAMPLE

The effect of the generalized Crank-Nicholson method when applied to a very simple problem is shown in Figure 6. The problem is a one-dimensional two-phase Buckley-Leverett type displacement. Typical values of fluid properties were chosen along with quadratic relative permeability curves with zero critical saturations. 20 grid blocks were used in the simulation. The figure shows the unit mobility ratio runs with the following parameters:

$\omega = 1.0 \quad \Delta S(t) = 2\%$

$\omega = 1.0 \quad \Delta S(t) = 20\%$

$\omega = 0.65 \quad \Delta S(t) = 20\%$

$\Delta S(t)$ is the average saturation change with the time step t. The results show a noticeable reduction in spatial truncation error with the generalized Crank-Nicholson method.

Table 1

Data for Oil Resaturation Problem

Reservoir Description

$L = 200$ ft	$H = 100$ ft	$W = 200$ ft
$k = 200$ md	$\phi = 0.3$	
$S_{wi} = 0.3$	$S_{oi} = 0.7$	$S_{gi} = 0.0$
$\mu_o = 5$ cp	$\mu_w = 1.0$ cp	$\mu_g = 0.02$ cp
$C_o = 16^{-6}$ psi^{-1}	$C_w = 0$ psi^{-1}	$C_r = 0$ psi^{-1}
$\varepsilon = 10^{-3}$	$c = 0.952$ (for the pseudo function)	
$P_i = 2100$ psig	$R_{si} = 1333$ scf/stb (i.e. undersaturated oil)	

Relative Permeability

$$k_{ro} = \left(\frac{S_o - 0.3}{1 - 0.3}\right)^2$$

$$k_{rg} = \left(\frac{S_g - 0.05}{1 - 0.05}\right)^2$$

PVT Data

P (psig)	R_s (scf/stb)	B_o (bbl/stb)	E_g (scf/bbl)	ρ_o (lb/ft^3)	ρ_g (lb/ft^3)
0	0	1	5.615	49.92	0.0765
3000	2000	2.25	1152		

PVT properties assumed linear between 0 and 3000 psi.

Well Data

$Q_I = 250$ stb/day dead oil

$$Q_p = \frac{2\pi k_r kh f}{\mu} \frac{(P_i - P_b)}{[\ln c_g r_e/r_w + S]}$$

where

$r_e = \sqrt{\frac{\Delta x \Delta y}{\pi f}}$ $\quad r_w = 0.5$ ft $\quad S = 0$

$P_b = 500$ psig $\quad f = 0.5$

$h = 20$ ft $\quad c_g = 0.543$

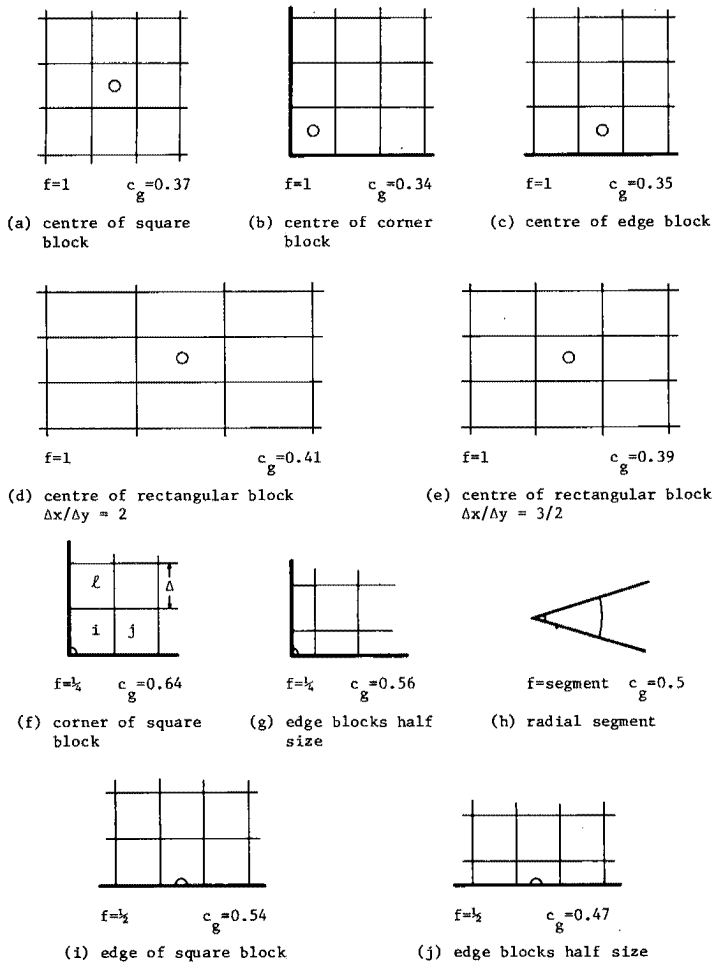

Fig. 1 - Geometrical Factor for Various Common Well Locations.

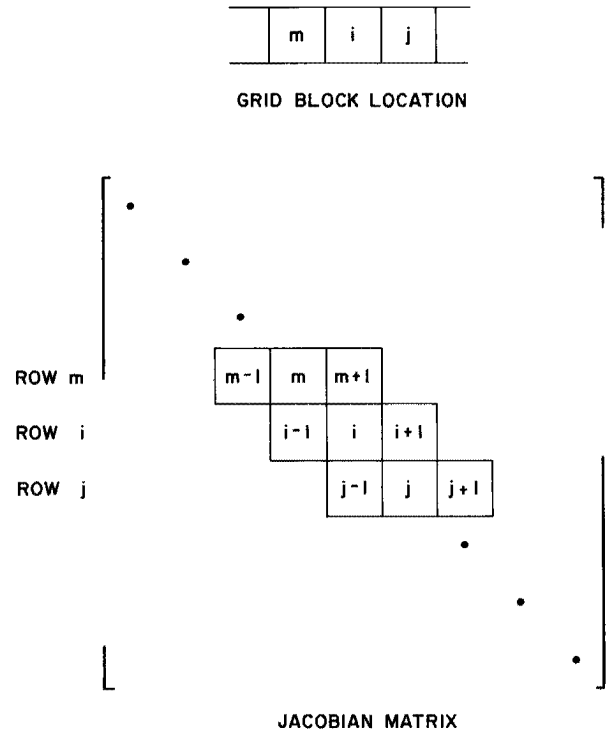

Fig. 2 - Jacobian Matrix Structure for a One-Dimensional Problem.

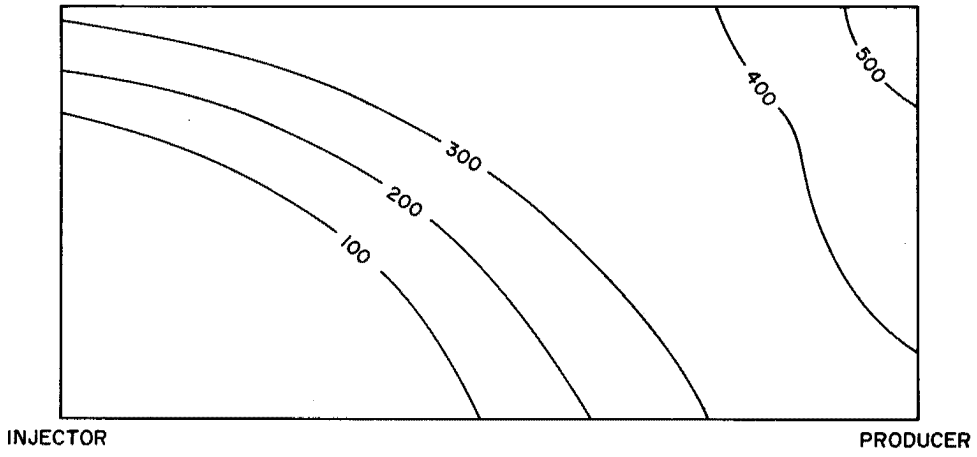

Fig. 3 - Contours of Solution Gas/Oil Ratio After 261 Days.

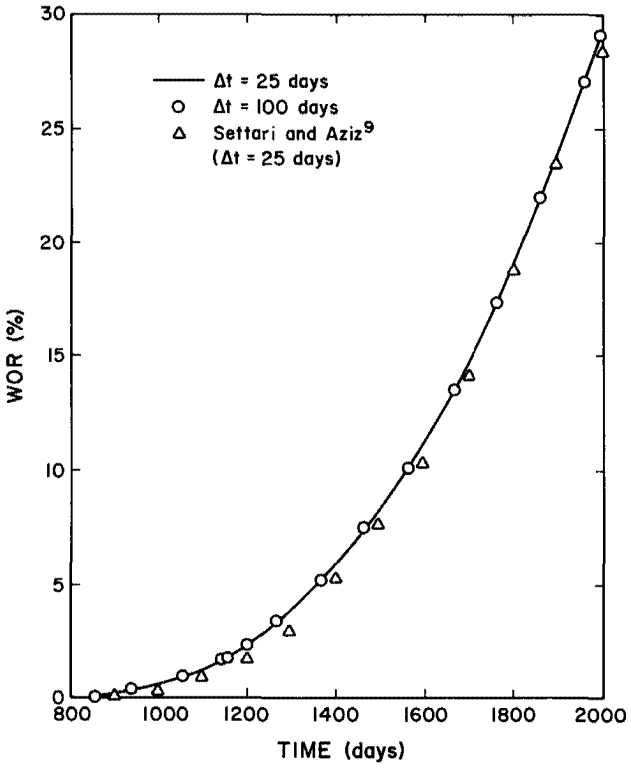

Fig. 4 - Water-Oil Ratio for the Water Coning Problem of Blair and Weinaug[8].

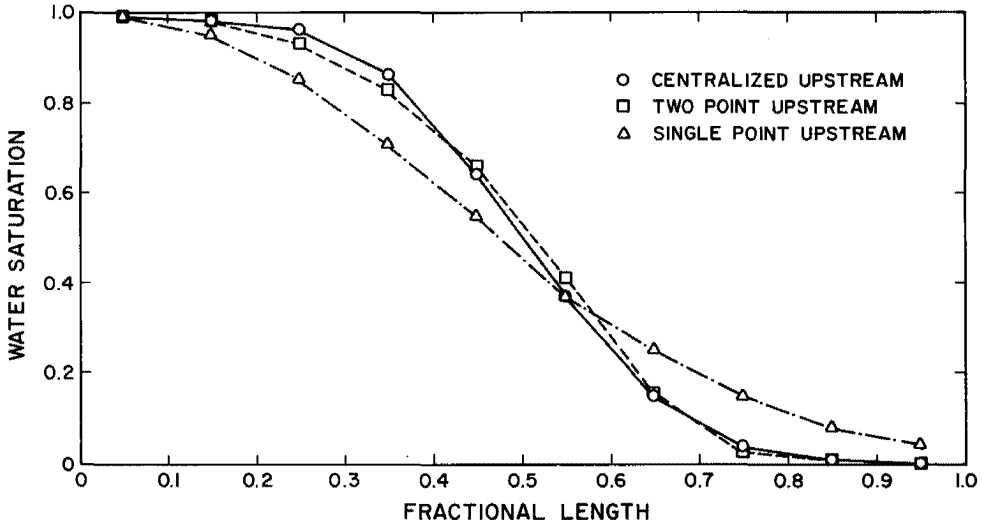

Fig. 5 - Water Saturation after 0.5 PV Injection for Three Mobility Approximation Schemes.

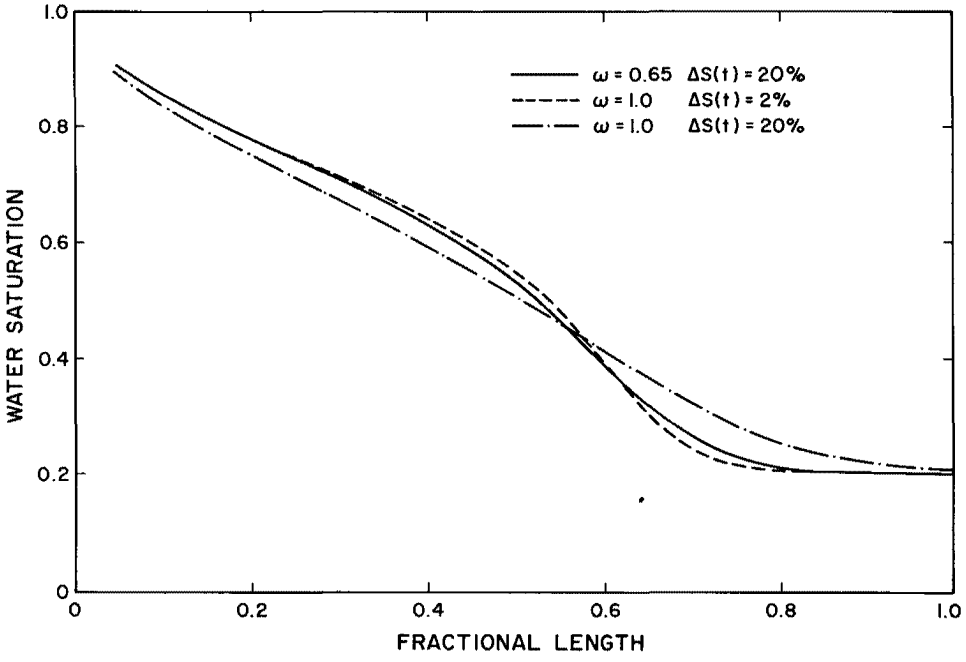

Fig. 6 - Water Saturation Profile Showing the Effect of Time Truncation.